Photovoltaic effects in porphyrin polymer films and heterojunctions

C. H. M. Marée, S. J. Roosendaal, T. J. Savenije, R. E. I. Schropp, T. J. Schaafsma et al.

Citation: J. Appl. Phys. **80**, 3381 (1996); doi: 10.1063/1.363203
View online: http://dx.doi.org/10.1063/1.363203
View Table of Contents: http://jap.aip.org/resource/1/JAPIAU/v80/i6
Published by the American Institute of Physics.

Photovoltaic effects in porphyrin polymer films and heterojunctions

C. H. M. Marée[a] and S. J. Roosendaal
Department of Atomic and Interface Physics, Utrecht University, Debye Institute, P.O. Box 80,000, 3508 TA Utrecht, The Netherlands

T. J. Savenije
Department of Molecular Physics, Wageningen Agricultural University, P.O. Box 8128, 6700 ET Wageningen, The Netherlands

R. E. I. Schropp
Department of Atomic and Interface Physics, Utrecht University, Debye Institute, P.O. Box 80,000, 3508 TA Utrecht, The Netherlands

T. J. Schaafsma
Department of Molecular Physics, Wageningen Agricultural University, P.O. Box 8128, 6700 ET Wageningen, The Netherlands

F. H. P. M. Habraken
Department of Atomic and Interface Physics, Utrecht University, Debye Institute, P.O. Box 80,000, 3508 TA Utrecht, The Netherlands

(Received 9 April 1996; accepted for publication 5 June 1996)

Electropolymerized porphyrin films on indium–tin–oxide substrates have been characterized using Rutherford backscattering spectrometry, absorption spectroscopy, electrical characterization methods and with step profiling. With these methods the density of the films ($\rho=1.35$ g/cm^3) and the absorption coefficients $\alpha(\lambda)$ have been determined. For film thicknesses exceeding 40 nm, silver electrical contacts without shunts are achieved by evaporation. The dark conductivity of the films amounts to 10^{-13}–10^{-12} Ω^{-1} cm^{-1}. When applying a band model for the conduction in the films, the dark space charge limited current and the exponent in the relation between photoconductivity and illumination intensity ($\sigma \sim I^{\gamma}$, $\gamma=0.65\pm0.05$) indicate an exponential trap distribution in the band gap of the films. From the action spectra, filter effects of the photoconductance and low mobilities are inferred. Spin coating of acceptor layers on top of the polymer films results in the formation of heterojunctions showing photovoltaic behavior, with an open-circuit voltage 0.4–0.6 V. The short-circuit current is controlled by electron transfer at the donor/acceptor interface only and is limited by filter effects in the bulk and by the low conductivity of the materials. The optoelectrical properties of the layers are different if analyzed using a mercury contact (higher dark conductivity, no photoconductivity) which is attributed to the introduction of dopants from ambient air in this case. [S0021-8979(96)00318-0]

I. INTRODUCTION

Recently, the application of organic dyes as light absorbing materials in organic solar cells and other photoelectric devices has gained considerable interest[1–3]. Organic dyes are potentially promising materials for use in solar cells: They exhibit high absorption coefficients, are inexpensive and are easily processed, and can be functionalized to obtain specific optical or electric properties. By selecting dyes with the appropriate redox potentials, heterojunctions of donor/acceptor layers have been produced which form a depletion layer and exhibit photovoltaic behavior[4,5].

The key role of chlorophyll (dihydroporphyrin) in natural photosynthesis has led us to the study of porphyrins as building blocks for organic solar cells. Electron transfer of donor–acceptor (D/A) complexes of water soluble porphyrins has been extensively studied and picosecond photoinduced electron transfer has been observed[6,7]. Several deposition methods for the formation of porphyrin thin films are available: vacuum sublimation;[8] spin coating;[9,10] formation of Langmuir–Blodgett films;[11] or dipcoating.[10,12] However, as the application of the layers in optoelectric devices requires homogeneous and pinhole-free films, only sublimation and chemical electropolymerization[13–15] seem successful methods to achieve a controlled layer growth.

The mechanism of electropolymerization of porphyrins and the photoelectric behavior of the films has been studied by Savenije, Koehorst, and Schaafsma.[16] These authors analyzed porphyrin polymer donor layers with different redox properties by varying the porphyrin metal center. By spin coating an acceptor layer on top of the electropolymerized donor layer, a heterojunction is formed. The observed photovoltaic effects were attributed to light-induced electron transfer from donor to acceptor rather than by the formation of a p–n junction. For the electric analysis of the layers a mercury back contact was used, which enabled measurement of very thin ($\leqslant 7$ nm) layers without shunts. The main drawback is that the experiments are performed in ambient air whereas the implementation of the films in photoelectric devices requires the use of solid back contacts. Therefore, here

[a]Electronic mail: maree@fys.ruu.nl

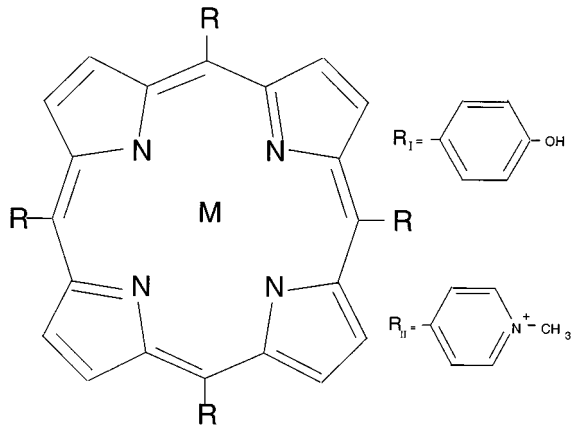

FIG. 1. Molecular structure of used porphyrins: $\mathbf{R}_I = C_6H_4OH$: hydroxyphenyl group; **M**=Zn, zinc tetra(4-hydroxyphenyl)porphyrin (ZnTHOPP); **M**=Pd, palladium tetra(4-hydroxyphenyl)porphyrin (PdTHOPP); $\mathbf{R}_{II}$, **M**=H_2, tetra(4-methyl pyridinium)porphyrin (H_2TMPyP).

we report on the photoelectronic properties of these layers which were measured using vacuum evaporated silver back contacts.

As the exact mechanism of the deposition of porphyrins by electropolymerization is still a subject of study, knowledge about the thickness and the composition of the layers is required. We therefore investigated the coverage and the thickness of the layers with Rutherford backscattering spectrometry (RBS) and step profiling, respectively. Also, the absorption characteristics of the dyes in the films may differ from the dyes in solution. Absorption characteristics of films with varying thickness are used to explain the photoelectric behavior of single polymer porphyrin layers and D/A heterojunctions. As intermolecular binding is weak in organic films, the overlap of the molecular orbitals is small which leads to low mobilities and the use of a band model to describe the electric behavior of molecular semiconductors may not be justified. However, many authors have successfully applied band models to describe electric aspects of organic films such as photoconductivity, trapping or junction formation.[9,17–23]

II. EXPERIMENT

A. Preparation

The purity of ZnTHOPP, PdTHOPP, and H_2TMPyP (Fig. 1) (Midcentury Chemicals) was checked by thin layer chromatography and absorption spectroscopy. The porphyrin layers were deposited on soda lime glass covered with a 70 nm conductive transparent In_2O_3:Sn (ITO) layer, R = 30 $\Omega/\square$ (Glastron), in order to allow optical and electric analysis of the films. Electropolymerization of donor-type dyes was carried out in a conventional three-electrode system with ITO as the working electrode.[24] $Ag/AgNO_3$ (3.0 M) was used as the reference electrode and a platinum wire as the counter electrode. The electropolymerization was carried out at room temperature from a 1 mM porphyrin solution in acetonitrile (MeCN) containing 0.1 M tetra tert-butyl ammoniumperchlorate as electrolyte and 0.05 M 2,6-di-tert.butylpyridinium added as base. The films were formed by cyclic polymerization. The potential was cycled between 0.0 and +1.0 V versus the reference electrode, with a scan rate of 0.1 V/s. After polymerization the films were rinsed with MeCN followed by washing in ethanol and drying with nitrogen. For details on the film growth we refer to Refs. 16 and 24.

Acceptor-type porphyrins films were deposited by spin coating a 1 mM H_2TMPyP solution in methanol at 3000 rpm on top of the first layer. Silver back contacts with a thickness of 0.3 μm and an area of 0.78 mm^2, were vacuum evaporated on top of the films at $\sim 1\times 10^{-4}$ Pa. In this way, 12 separate cell structures consisting of ITO, dye layer(s) and silver contact were formed on each sample For porphyrin films thinner than $\sim$40 nm, the structures with silver contacts were all short circuited due to pinholes. At film thicknesses of 50 nm, about half of the structures were shunted and the number of shunts decreased even more for thicker films.

B. Analysis

RBS measurements were performed with a 2.0 MeV He^+ beam from a 3 MV Van de Graaff accelerator. The beam was collimated to a beam spot of ~ 1 mm^2. The scattering angle was 170°, the incident beam angle with the sample surface was 25°, and the exit angle is 15°.

The thickness of the films was measured by step profiling (Dektak 3030) mechanically made grooves in the film. Absorption measurements were done with a spectrophotometer (Perkin–Elmer) in combination with a diffuse integrating sphere. Total transmission and reflectance spectra were recorded and the absorption spectra were corrected for reflectance and interference effects.

The photoconductivity and photovoltaic effects of the films were measured between the ITO layer as front and the Ag layer as external back contact, using an Oriel solar simulator appropriately filtered and calibrated to obtain global AM1.5 irradiation. The photoresponse times of the porphyrin cells were long, ranging from several seconds to several minutes; therefore, measurements with a lock-in amplifier were not feasible and the measurements were mostly made in dc mode. The light intensity was varied by 18 neutral density filters from 16 to 100 mW/cm^2. Interference filters with a bandwidth of $\sim$10 nm were used for spectral response measurements.

III. RESULTS

A. Characterization of the films

RBS was applied for the analysis of films of a single type of porphyrin, as well as the D/A heterojunctions. Previously, we reported on the analysis of the coverage and composition of zinc porphyrin layers and their stability to ion-beam-induced damage.[25] It was noted that all constituents of the film, except for hydrogen, remained stable in the layers during RBS analysis. Furthermore, it was observed that the stoichiometry of the porphyrin molecules was reflected in the composition analysis of the layers. Some additional hydrogen and chloride were found present in the layers, however, indicating that some electrolyte is incorporated in the films.

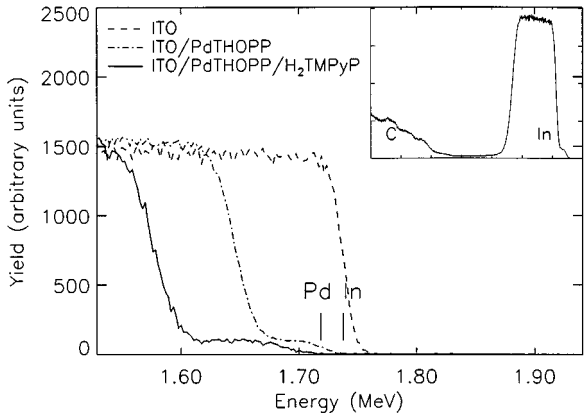

FIG. 2. RBS spectra of the indium edge of bare ITO and ITO substrates covered with a PdTHOPP single film and a H_2TMPyP/PdTHOPP A/D heterojunction film. In the inset the total RBS spectrum of the single porphyrin film is shown (2.0 MeV He, $\theta=170°$ and $\alpha=25°$).

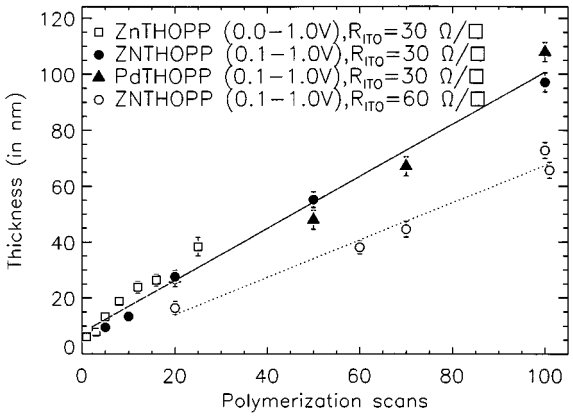

FIG. 4. Thickness of various polymer layers vs the number of polymerization scans.

The RBS measurements were performed in a glancing geometry, which enables better depth resolution due to the increased length of the inward and outward path of the He ion.[26]

In Fig. 2, the RBS spectrum of a PdTHOPP/H_2TMPyP (D/A) heterojunction on an ITO-coated substrate is shown. The total coverage has been determined from the shift of the indium substrate edge, using the energy loss of helium calculated with the previously determined film composition.[25] The shift of the palladium edge indicates the coverage of the polymer layer by the spin-coated acceptor.

In Fig. 3 the total atomic coverage of single donor films is depicted versus the thickness determined from step profiling. From the slope we obtain the following empirical relation between coverage G (atom/cm^2) and the thickness d (nm):

$$G=(8.83\pm 0.13)\times 10^{15}\ d. \tag{1}$$

Using Eq. (1), we can also express the molecular coverage Γ (in grammol/cm^2) versus thickness d (in nm):

$$\Gamma=(1.81\pm 0.03)\times 10^{-10}\ d. \tag{2}$$

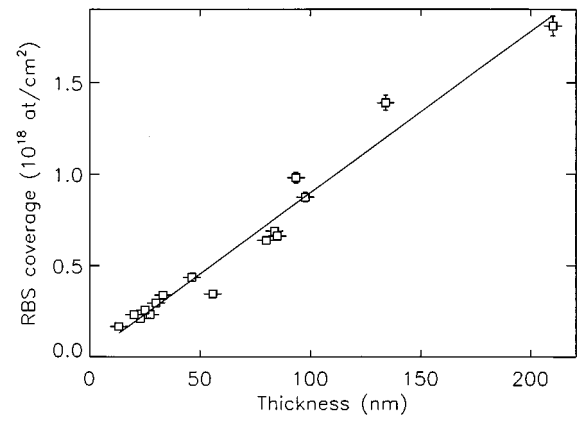

FIG. 3. Total atomic coverage as determined with RBS vs profilometric thickness.

The experimentally obtained density ($\rho=1.35$ g/cm^3) is somewhat less than the density deduced from the dimension of the molecules, $1.5\times 1.5\times 0.35$ nm^3 (1.56 g/cm^3). Also, spin-coated layers were analyzed with RBS and the step profiler. The average coverage is 250×10^{15} atoms/cm^2 and the H_2TMPyP acceptor layers are $\sim$22 nm thick.

Using relation (1) in combination with RBS measurements, the growth rate of the porphyrin films has also been determined (Fig. 4). Although differences in experimental conditions probably influence the film growth (e.g., aging of porphyrin solution, position of the ITO electrode, mixing of the solution) a general trend is observed. During the first scan a porphyrin film of 5–7 nm is deposited. After this first fast growth, the growth rate decreases to about 0.8 nm/scan. The growth rate may be negatively affected by low conductance of the electropolymerized layers or the ITO substrate, as is inferred from Fig. 4; however, no limitation of the total thickness has been found so far.

The UV–VIS absorption of the porphyrin films shows that both the Soret band as well as the Q band are broadened with respect to the porphyrins in solution. The optical density (OD) of the main absorption peaks is linearly correlated with the film thickness (Fig. 5), indicating that the absorption coefficient per polymerized layer is independent of the film thickness. Therefore, the extinction coefficient $\epsilon(\lambda)$ and, using Eq. (1), the absorption coefficient $\alpha(\lambda)$ (cm^{-1}) has been determined by averaging the absorption spectra at various film thicknesses. The transmission of light in a film of thickness d is given by

$$I(d,\lambda)=I_0 10^{-\epsilon(\lambda)\Gamma}=I_0 e^{-\alpha(\lambda)d}. \tag{3}$$

Figure 6 shows the absorption coefficient $\alpha(\lambda)$ vs λ for PdTHOPP polymer. The values for $\alpha(\lambda)$ are somewhat lower than the extinction coefficient of PdTHOPP in solution [from the extinction coefficient of the Soret band in solution (2.26×10^5 ℓ/mol cm) a value for α at $\lambda=430$ nm of 90 μm^{-1} is calculated]. Figure 6 and Eq. (1) yield a direct relation between absorption, atomic coverage and thickness of the polymer films, which is used for the optoelectric analysis of the films.

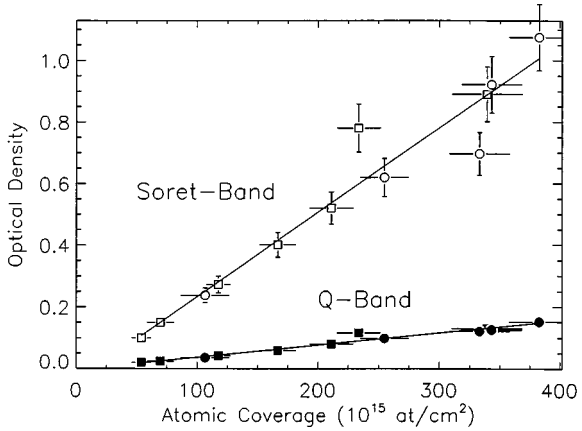

FIG. 5. Optical density of the maximum of the Soret band (○) and Q band (●) for two polymer porphyrin layers vs RBS atomic coverage: (1) □ ZnTHOPP; (2) ○ PdTHOPP.

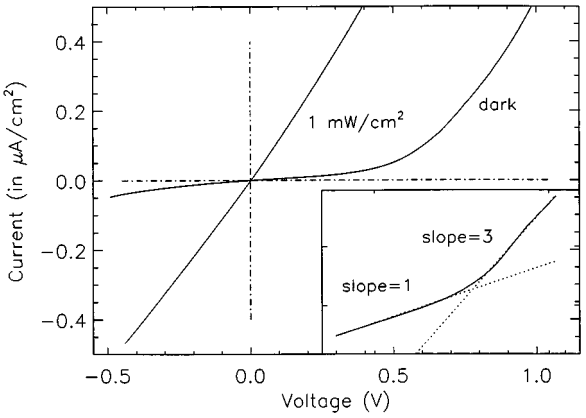

FIG. 7. I–V curves of a 100 nm single ZnTHOPP film in the dark and under 1 mW/cm^2 AM1.5 illumination. In the inset the dark curve of log(I) vs log(V) shows the transition from linear to supralinear behavior.

B. Single porphyrin layers

In Fig. 7, typical current–voltage (I–V) measurements of polymer donor layers are shown. A positive voltage indicates a positive voltage on the silver back contact. The dark currents are nonlinear. On a double logarithmic scale the curves can be separated in a linear part, I$\sim$V (V$<$0.35 V) and a supralinear behavior for voltages exceeding V$\simeq$0.35 V, given by I$\sim$V^m (m=2.5–3.0). The dark conductivity in the ohmic part amounts to 10^{-12}–10^{-13} Ω^{-1} cm^{-1}. The curves are almost point symmetrical with respect to V=0 V, although the PdTHOPP films show some rectifying effect toward the ITO contact. Upon low-intensity illumination (1 mW/cm^2), the I–V curves of the layers are completely linear in the applied measurement range (−1.0–1.0 V), thus the layer and the two contacts appear to be ohmic. Also, no photocurrent is observed upon illumination, which suggests that no significant contact barrier at either electrode has formed.

Figure 8 shows the photoconductivity of the films. Between dark and 100 mW/cm^2 (AM1.5) illumination an increase of the conductivity over three orders of magnitude is noted. It is noteworthy that the same measurements using a mercury back contact did not reveal any significant dependence of the resistivity of the layers on the illumination intensity.[16]

The dependence of the photoconductivity σ_{ph}, on the illumination intensity F is generally given by the relation[18,27]

$$\sigma_{ph}=F^{\gamma}. \tag{4}$$

We have found a value for γ of 0.65±0.05 (ranging from 0.60 to 0.75) over the complete intensity range studied for both the ZnTHOPP and PdTHOPP films. Values for $0.5<\gamma<1.0$ are commonly associated with photocarrier lifetimes determined by trapping centers.

The emission of photocarriers from traps is observed when we measure the photoconductivity transient after switching off the light source.

In Fig. 9 a fast initial recombination of charge carriers is observed, followed by a slow decay, which extends to several minutes. The characteristic time of the slow decay is independent of prior illumination intensity for light intensities above ~1 mW/cm^2. We conclude that at (light) intensities larger than ~1 mW/cm^2 all relevant traps are filled by the photogenerated charge carriers. After switching off the light source, the trapped carriers are thermally emitted from

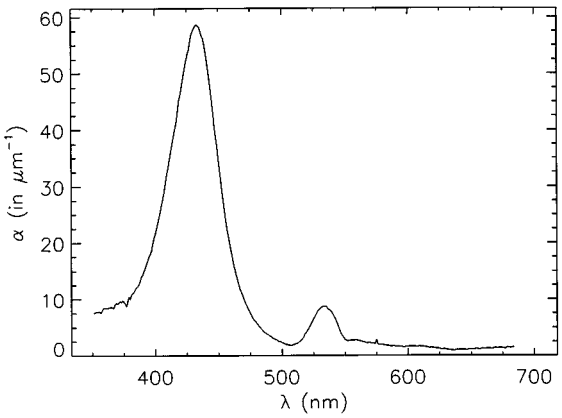

FIG. 6. Absorption coefficient $\alpha(\lambda)$ vs λ for PdTHOPP films.

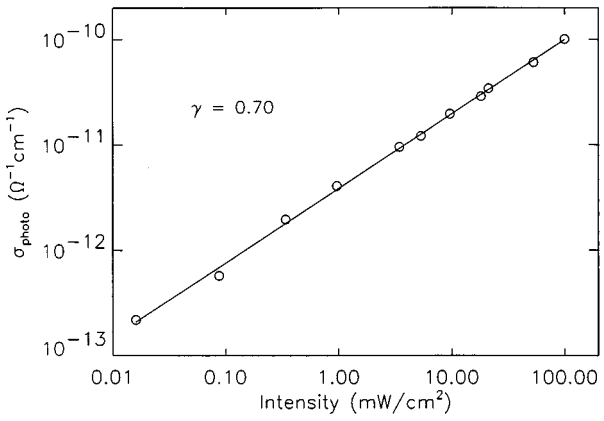

FIG. 8. Logarithmic curve of conductivity vs illumination intensity of a 100 nm ZnTHOPP film.

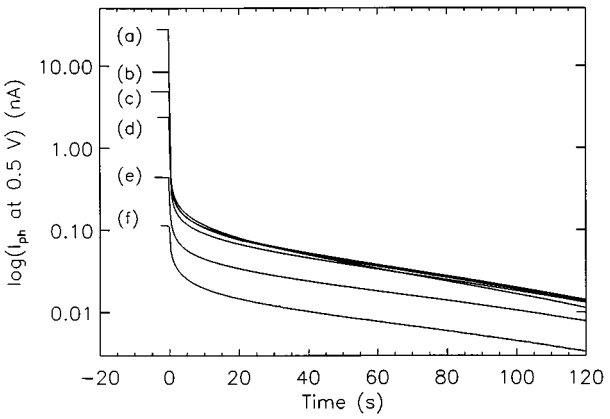

FIG. 9. Transient of the current at +0.5 V of a ~90 nm PdTHOPP single layer after switching off the light at various intensities. (a) 100 mW/cm^2; (b) 21 mW/cm^2; (c) 10 mW/cm^2; (d) 3 mW/cm^2; (e) 0.3 mW/cm^2; (f) 0.1 mW/cm^2.

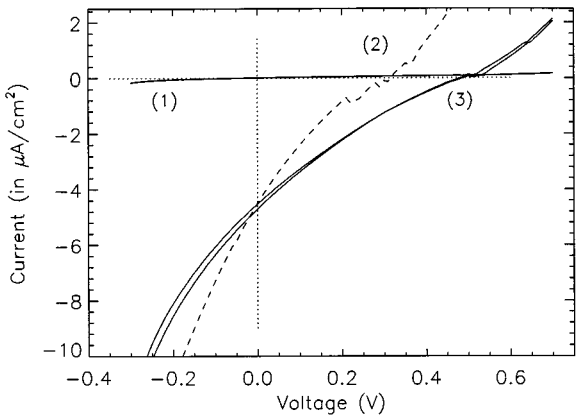

FIG. 11. I–V curves of a ITO/PdTHOPP(130 nm)/H_2TMPyP(25 nm)/Ag heterojunction in dark and under 100 mW/cm^2 (AM1.5) illumination. Voltage scans (from -V to +V) are made at different speeds. (1) Dark curve; (2) voltage scan 0.01 V/s; (3) voltage scan 0.001 V/s.

the deep traps. If the lifetime of the emitted carriers is dominated by bimolecular carrier recombination the photoconductivity is given by[18]

$$\sigma_1 = \frac{\sigma_{\mathrm{ph},0}}{k_d(t+1)}, \quad \sigma = \sigma_{\mathrm{ph}} + \sigma_{\mathrm{dark}}. \tag{5}$$

Here $\sigma_{\mathrm{ph},0}$ is the conductivity at the end of the illumination caused by trapped carriers. Apart from the fast initial decay, which we ascribe to geminate recombination, a good fit of Eq. (5) to the curves in Fig. 9 was found for $t>5$ s. A time constant for carrier recombination as large as $k_d=0.015 \pm 0.002$ s^{-1} is found. We suggest that the slow decay and long photocarrier lifetime are associated with low carrier mobilities.

The spectral response of the photoconductivity for ~50 nm layers agrees with the absorption of the films, i.e., the photoconductivity peaks at the Soret and Q-band positions, although the spectral response of the Soret band is lower with respect to the Q-band (ratio ~3:1) than is expected from the absorption ratios (see Fig. 6). In Fig. 10 the spectral dependence of a 90 nm PdTHOPP film shows deviations of this pattern. Instead of a photoconductivity maximum at the Soret band position, a minimum in conductivity is observed at 420 nm for this and other, thicker, layers. This minimum is attributed to absorption filter effects of the film which are reflected in the photoconductivity.

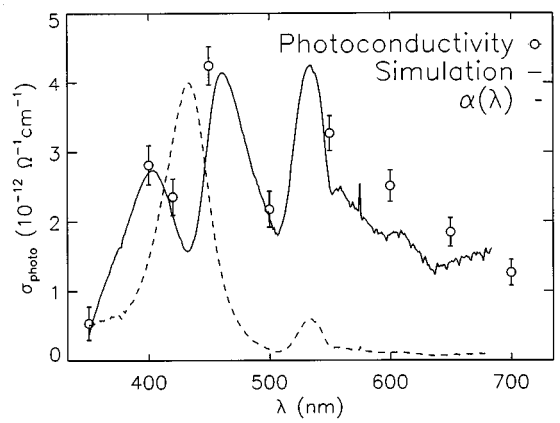

FIG. 10. Action spectrum of the photoconductivity of a ~90 nm PdTHOPP film. The calculated action spectrum, Eq. (15), and the absorption spectrum are scaled to the measured conductivity.

C. Acceptor/donor heterojunctions

We studied a range of ITO–(Pd/Zn)THOPP–H_2TMPyP–Ag heterojunctions, illuminated from the ITO electrode side for various thickness of the polymer. Figure 11 shows I–V curves in the dark and 100 mW/cm^2 (AM1.5) illumination. For accurate measurements the slow response of the heterojunction to voltage changes has to be taken into account. In the dark, no strong rectifying effect between the layers is observed. Further, we observed an external photocurrent which is directed from the ITO to the silver contact, indicating that photoinduced injection of electrons from the polymer donor layer to the spin coated acceptor layer causes the photovoltaic behavior. Thus, we conclude that no significant $p-n$ junction is formed in the dark, in accordance with the conclusions of Ref. 16. The fill factor (FF) of the I–V curves in all measurements is close to 0.25; however, the response time of the current to changes in voltage can be on the order of several seconds (in contrast to the case in Ref. 16), as is shown in Fig. 11. We therefore measured the short-circuit current and open-circuit voltage after the cells were stabilized. Figure 12 shows the increase of the short circuit current I_{sc} versus light intensity F. Using the relation $I_{sc} = F^m$, m values varying from 0.75–0.90 were found in the films. The open-circuit voltage V_{oc} of the cells increases rapidly with the light intensity and saturates at a value of 0.4–0.6 V for $F>1$ mW/cm^2, which is somewhat higher than the V_{oc} obtained with Hg contacts.[16]

The action spectrum of I_{sc} is similar to the absorption spectrum (Fig. 6) for layers 40–50 nm thick. However, if the polymer layer is thicker, a photoaction minimum is found at the position of the Soret band. Figure 13 shows this minimum, which indicates filtering of the light in the bulk of the polymer film. Apparently, no significant energy transfer from

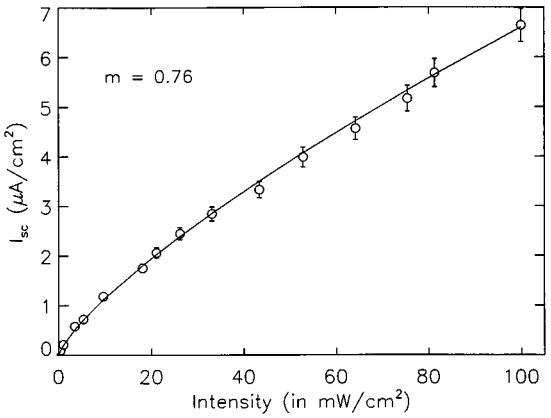

FIG. 12. Short-circuit current I_{sc} of an ITO/PdTHOPP(130 nm)/H_2TMPyP(25 nm)/Ag heterojunction vs illumination intensity.

photons absorbed in the bulk of the donor to the D/A interface occurs. In Fig. 13 the spectral response measured with a 3 Hz lock-in amplifier and a 2 nm monochromator is shown for comparison; however, absolute measurements were not feasible with the lock-in technique, due to the slow response of the cells.

IV. DISCUSSION

A. Comparison of the mercury and silver contacts

We compared optoelectric experiments on polymer porphyrin layers, using a solid silver back contact, with the experiments using mercury back contact, reported by Savenije and co-workers.[16] This comparison shows remarkable differences in behavior. We suggest that the absence of significant photoconductivity effects and the much higher dark conductivity ($\sim 10^{-7}\ \Omega^{-1}\ \mathrm{cm}^{-1}$) with the mercury contacts is ascribed to the effect of unintentional dopants. It is known that the organic semiconductor properties can be varied over many orders of magnitude by doping effects, e.g., by O_2 or H_2O incorporation.[17,28] The analysis of the films with the mercury contacts is done in air and thus the incorporation of these dopants in the films is conceivable. Vacuum evaporation of Ag may have led to depletion of dopants from the film. We find that the photoinduced carrier concentration in the Ag-sealed films upon maximum illumination (100 mW/cm^2) is still lower than the dark carrier concentration of the films in air.

The sealing effect of Ag is further confirmed by remeasuring the conductivity of the structures after keeping them for 1 year in ambient on the shelf. No significant changes in the optoelectric properties have been found, whereas the structures with mercury contacts deteriorate within 1 month. Thus, no apparent indiffusion of dopants after encapsulating by the silver occurs and we conclude that stable and reproducible devices may be produced in this manner.

We do not ascribe the observed differences to effects of varying contact interfaces or to differences in the work function of the materials, since no indication of non-ohmic contacts in either case was found. Furthermore, no significant differences in electronic properties are observed in the films, using evaporated copper, instead of silver, contacts. And as the work function of mercury is between Ag and Cu (Φ_{Ag}=4.26, Φ_{Hg}=4.49, Φ_{Cu}=4.65 eV),[29] we conclude that the differences are not caused by work-function differences.

Although our observations on the single films as well as D/A heterojunction are in general agreement with the observations reported in Ref. 16, the implication is that for application of these organic films in devices, special precautions have to be taken with regard to dopant incorporation. Especially carrier concentrations and transient times may be significantly altered due to these effects.

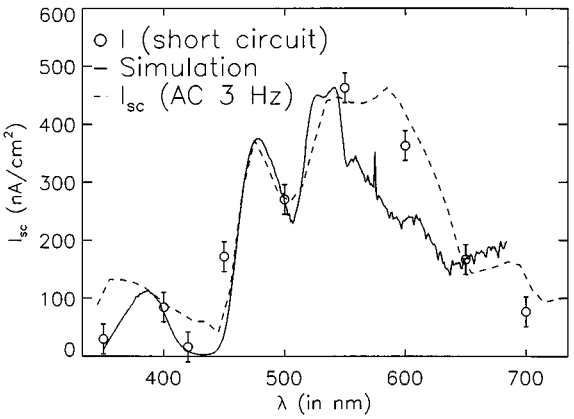

FIG. 13. Photoaction spectrum of a PdTHOPP/H_2TMPyP heterostructure. The data are fitted to Eq. (16). A photoaction spectrum measured using a monochromator and a lock-in amplifier at 3 Hz is scaled to the spectrum measured with filters.

B. Photoconductivity

Due to the low mobilities found in organic semiconductors, varying from 1 cm^2/V s in single crystals to 1×10^{-6} cm^2/V s in polymers, many authors use hopping or tunneling models to describe the electric properties of these materials.[17,19] However, we discuss the observed photoconductance effects following the band model of conductivity in organic materials of Meier,[18] as this model provides a good description of our experimental results. The band model is often applicable in organic semiconductors, although, e.g., the activation energies determined from the temperature dependence of conduction (determined by hopping), from the photoconductivity, and from the absorption spectrum are not equal and do not reflect a forbidden energy zone as is the case in inorganic materials.

The dependence of photoconductivity on light intensity is given by γ in Eq. (4) which varies from 0.60 to 0.75. A value for γ lower than 1.0 is commonly associated with the presence of trap centers within the band gap. The low γ values indicate a continuous, exponential distribution of trapping centers, $N(E)$ ($\mathrm{cm}^{-3}\,\mathrm{eV}^{-1}$), which may be expressed by

$$N(E)=\frac{N_t}{kT_c}\exp\left(-\frac{E}{kT_c}\right). \tag{6}$$

T_c is a parameter which indicates the steepness of the distribution, N_t is the total trap density, and E is the energy dif-

ference of the trapping level with the band edge. From Eq. (6) the expression for the concentration of free photocarriers n is deduced,[18]

$$n=(f\tau N_c^{T/T_c})^{T_c/(T_c+T)}. \tag{7}$$

The generation rate f is supposed to be proportional to the number of absorbed photons per second ($f\sim F$), N_c is the density of states in the conduction band, and τ is the lifetime of the photocarriers, determined by the number of traps ($\tau\sim 1/N_t$). Equations (7) and (4) yield the relation

$$\gamma=T_c/(T_c+T). \tag{8}$$

Thus, for $\gamma=0.65\pm0.05$ at room temperature, we calculate for T_c, which describes the trap distribution, $T_c=540\pm100$ K.

The dark I–V curves of the polymer films show a transition from ohmic behavior to supraquadratic behavior. This is caused by the low concentration of charge carriers. If the voltage is high enough carriers are injected from the contacts into the film and a space-charge layer is formed, which results in a space-charge-limited current (SCLC). If the carrier concentration is increased by photoabsorption, the transition voltage to SCLC increases. In our measurements, low light intensities already cause shifts of the transition voltage outside the measurement range. The magnitude of the SCLC is determined by the presence and filling of traps. If the trap density has an exponential distribution [Eq. (6)], the dependence of the current I on voltage and film thickness d is given by[18]

$$I\sim\frac{V^{(T_c/T)+1}}{d^{2(T_c/T)+1}}. \tag{9}$$

For the values for $m=2.7\pm0.2$ we calculate a characteristic temperature of $T_c=500\pm40$ K. Therefore, we conclude that a description in terms of an exponential trap distribution is adequate, as the independent measurements of the SCLC in the dark and the intensity dependence of the photoconductivity γ give similar results. The comparatively low value of T_c indicates a steep energy distribution of the traps in these porphyrin films.

In general, the photoconductivity is expressed by the following equation:

$$\sigma_{\rm ph}=q\mu n. \tag{10}$$

Here n is the concentration of photocarriers and the mobility is given by μ, which is related to the microscopic mobility μ_0 by[18]

$$\mu=\frac{n_{\rm free}}{n_{\rm free}+n_{\rm trapped}}\mu_0=\Theta\mu_0. \tag{11}$$

n refers to the concentration of majority carriers. However, we do not know whether electrons or holes are the major carriers, so n is replaced by p in the latter case. The charge carrier density generation rate $\mathscr{F}$ ($\mathrm{cm^{-3}\,s^{-1}}$) in inorganic materials is frequently expressed as the integrated photogeneration rate, averaged over the layer thickness,[27]

$$\mathscr{F}=\frac{\int_0^d f(x)\,dx}{d}=\frac{\int_0^d C\alpha(\lambda)e^{-\alpha(\lambda)x}\,dx}{d}$$
$$=\eta N_{\rm ph}(1-R)\left(\frac{1-e^{-\alpha(\lambda)d}}{d}\right), \tag{12}$$

with $N_{\rm ph}$ the number of incident photons ($\mathrm{cm^{-2}\,s^{-1}}$), R the reflection coefficient, d the thickness of the film, and α the absorption coefficient. The quantum efficiency η is the number of created free carriers in the porphyrins per absorbed photon. The value of η depends on possible decay processes of the excited porphyrin molecule (e.g., fluorescence, nonradiative decay). In the treatment (10)–(12) the concentration of photogenerated carriers is averaged over the total layer thickness; however, this averaging does not result in the dip in the conductivity at the wavelength of maximum absorption of the porphyrins, which is observed in Fig. 10.

However, if the charge carriers are not very mobile the overall resistivity of the films must instead be calculated from the series resistance of the different slabs of the films, each with their own absorption, generation rate, and, thus, concentration of photocarriers. We therefore assume that the overall conductivity is determined by the integral of the local resistivity (determined by the local photocarrier concentrations), rather than averaging the total amount of formed photocarriers over the total film thickness as is the case for high mobilities. Analogue to Gregg, Fox, and Bard,[30] we deduce for the conductivity σ

$$\sigma=\frac{1}{\int_0^d\{1/q\mu[n(x)]\}dx}. \tag{13}$$

$n(x)$ is the local photocarrier concentration at depth x from the illuminated ITO electrode, given by Eq. (7). The electron generation rate $f(x)$ is given by

$$f(x)=\eta N_{\rm ph}(1-R)\alpha(\lambda)e^{-\alpha(\lambda)x}. \tag{14}$$

We use Eqs. (7) and (14) to evaluate the integral in Eq. (13), in which we consider the local carrier density $n(x)$. Then it follows that the spectral response of the photoconductivity $\sigma(\lambda)$ is given by

$$\sigma(\lambda)=q\mu(\eta\tau N_c^{1/\gamma-1})^{\gamma}\{[1-R(\lambda)]N_{\rm ph}(\lambda)\}^{\gamma}$$
$$\times\frac{\gamma\alpha^{\gamma+1}(\lambda)}{e^{\gamma\alpha(\lambda)d}-1}. \tag{15}$$

In Fig. 10 the theoretical $\sigma(\lambda)$ is compared with the experimental action spectra and a good qualitative agreement is found. In the calculation we used the values of $\alpha(\lambda)$ as given in Fig. 6, d=90 nm and $\gamma=0.65$. $N_{\rm ph}$ is taken equal to the spectral output of solar simulator plus filters and $R(\lambda)$ is taken from the spectral reflection data. We conclude that the results of the action spectra validate the model in which low carrier mobilities cause differences in local free carrier densities and thus influence the overall conductivity.

The explanation is thus found in the very low mobility of carriers in organic materials.[17,18,30] A value as low as 8×10^{-9} $\mathrm{cm^2/V\,s}$ for the effective mobility is inferred by Savenije and co-workers[24] from measurements of the diffusion coefficient of carriers in the porphyrin polymer films.

Though the actual mobility depends on the effective mobility and the number of traps [Eq. (11)], a low mobility is expected in this material. The somewhat higher conductivity (than expected from the model) for large wavelengths may be ascribed to reflection at the silver back contact causing multiple path lengths of the less absorbed light at these wavelengths.

C. Photovoltaic effects

The photovoltaic effects found in the cells with silver back contact are in qualitative agreement with the experiment on D/A heterojunction with a mercury contact,[16] although in the present article thicker layers (50–150 nm) have been studied. It is concluded that only electron transfer at the direct interface of the donor and acceptor layers contributed to the photocurrent, as the I_{sc} decreased nonexponentially with the thickness of the polymerized layer and also from the direction of the photocurrent which makes the presence of a space-charge layer not probable.

The observed photocurrent action spectra (Fig. 13) underline this conclusion. If the photocurrent is determined by interfacial absorption and charge transfer the following relation is expected:

$$I_{sc}(\lambda) = \eta[1 - R(\lambda)]N_{ph}(\lambda)(\Delta d)\alpha(\lambda)e^{-\alpha(\lambda)d}. \quad (16)$$

The distance of the interface to the illuminated ITO electrode is given by d and the width of the active region by Δd. The quantum efficiency for charge separation in this layer is given by η. The fit of this model to the experimental data (Fig. 13) yields a width of the active region of 3 Å if we take $\eta = 1$ in this layer. Thus, the absorption by a single D/A bilayer is sufficient to produce the measured photocurrents. The total efficiency of the cells is smaller than the values found in Ref. 16. This cannot solely be explained by the increased filtering effects in the bulk of the thicker polymer films but is probably also due to the higher resistance of the layers caused by the absence of doping. The I_{sc} dependence on the illumination intensity with values for the exponent lower than one further indicates the influence of film series resistance on the photovoltaic effect.

V. CONCLUSIONS

We have shown that dense, homogeneous porphyrin films with thicknesses 5–200 nm can be formed on ITO (In_2O_3:Sn) by electropolymerization. Control of the film thickness is achieved by measuring the coverage with RBS. Combination of RBS data with step profiling and absorption experiments yield the density of the films ($\rho = 1.35$ g/cm^3) and $\alpha(\lambda)$ curves. Thus, the film thickness can be determined by measuring the absorption or visa versa.

We performed optoelectric measurements on the polymer films by employing evaporation of silver back contacts. A sublinear dependence of the photoconductivity on the light intensity has been observed. From these measurements and from analysis of the dark SCLCs, we infer the presence of an exponentially distributed trap density toward the band edge, characterized by a characteristic temperature $T_c \sim 500$ K. Previously, higher dark conductivity and no photoactivity were found in the same type of layers which were made with mercury back contacts.[16] We attribute this difference to the incorporation of dopants from air into the films in the latter case. The action spectra of the photoconductivity indicate that the carrier creation and recombination are localized due to low mobility of the carriers in the film. This results in filter effects influencing the spectral response of the conductivity.

Starting with the polymer porphyrin films, D/A heterojunctions were formed and photocurrents were observed; however, the photoinduced charge separation is confined to the interfacial layer and no space-charge layer appeared to be formed in the dark. The high resistivity of the films in combination with filter effects and the small photoactive region limit the applicability of the studied films for optoelectric devices. Antenna layers exhibiting better conduction properties as well as energy absorption and transfer to the charge separating interface should be pursued to improve the performance.[9,11,31,32]

ACKNOWLEDGMENTS

The authors wish to thank the crew of the van de Graaff laboratory for running the accelerator. This work is supported by the Dutch Agency for Research on Energy and Environment (NOVEM), Netherlands, and the Dutch Foundation for Chemical Research (SON) with financial aid of the Dutch Organization for Scientific Research (NWO).

[1] M. K. Nazeeruddin, A. Kay, I. Rodrico, R. Humphrey-Baker, E. Müller, P. Liska, N. Vlachopoulos, and M. Grätzel, J. Am. Chem. Soc. **115**, 6382 (1993).
[2] T. A. Heimer, C. A. Bignozzi, and G. J. Meyer, J. Phys. Chem. **97**, 11 987 (1993).
[3] A. Hagfeldt, B. Didriksson, T. Palmqvist, H. Lindström, S. Sodergren, H. Rensmo, and S.-E. Lindqvist, Sol. Energy Mater. Sol. Cells **31**, 481 (1994).
[4] S. Günster, S. Siebentritt, and D. Meissner, Mol. Cryst. Liq. Cryst. **230**, 351 (1993).
[5] K. Takahashi, S. I. Nakatani, T. Matsuda, H. Nambu, T. Komura, and K. Murata, Chem. Lett. **11**, 2001 (1994).
[6] F. J. Vergeldt, R. B. M. Koehorst, T. J. Schaafsma, J. C. Lambry, J. L. Martin, D. G. Johnson, and M. R. Wasielewski, Chem. Phys. Lett. **182**, 107 (1991).
[7] U. Hofstra, R. B. M. Koehorst, and T. J. Schaafsma, Chem. Phys. Lett. **144**, 125 (1986).
[8] Y. Harima, M. Miyatake, and K. Yamashita, Chem. Phys. Lett. **200**, 263 (1992).
[9] B. A. Gregg and Y. I. Kim, J. Phys. Chem. **98**, 2412 (1994).
[10] J. Wienke, F. Kleima, R. B. M. Koehorst, and T. J. Schaafsma, in *Proceedings of the 12th EPSEC* (H.S. Stephens & Associates, Bedford, U.K., 1994).
[11] J. M. Kroon, P. S. Schenkels, M. van Dijk, and E. J. R. Sudhölter, J. Mater. Chem. **5**, 1309 (1995).
[12] A. Kay and M. Grätzel, J. Phys. Chem. **97**, 272 (1993).
[13] E. M. Baum, H. Li, T. F. Guarr, and J. D. Robertson, Nucl. Instrum. Methods Phys. Res. B **56**, 761 (1991).
[14] A. Guiseppi-Elie, S. R. Pradhan, A. M. Wilson, D. L. Allara, P. Zhang, R. W. Collins, and Y. T. Kim, Chem. Mater. **5**, 1474 (1993).
[15] G. Ramachandraiah, F. Bedioui, J. Devynck, M. Serrar, and C. Bied-Charreton, J. Electroanal. Chem. **319**, 395 (1991).
[16] T. J. Savenije, R. B. M. Koehorst, and T. J. Schaafsma, Chem. Phys. Lett. **244**, 363 (1995).
[17] J. Simon and J. J. André, *Molecular Semiconductors* (Springer, Berlin, 1985).
[18] H. Meier, *Organic Semiconductors: Dark and Photoconductivity of Organic Solids* (Verlag Chemie, Weinheim, 1974).

[19] D. Adam, F. Closs, T. Frey, D. Funhoff, D. Haarer, H. Ringsdorf, P. Schuhmacher, and K. Siemensmeyer, Phys. Rev. Lett. **70**, 457 (1993).
[20] A. Bertram, K. Engel, S. Siebentritt, S. Günster, R. Hiesgen, and D. Meissner, in *Proceedings of the 12th EPSEC* (H. S. Stephens & Associates, Bedford U.K., 1994).
[21] H. Bötcher, T. Fritz, and J. D. Wright, J. Mater. Chem. **3**, 1187 (1993).
[22] D. Wöhrle, L. Kreienhoop, G. Schnurpfeil, J. Elbe, B. Tennigheit, S. Hiller, and D. Schlettwein, J. Mater. Chem. **5**, 1819 (1995).
[23] G. Yu, J. Gao, J. C. Hummelen, F. Wudl, and A. J. Heeger, Science **270**, 270 (1995).
[24] T. J. Savenije, R. B. M. Koehorst, and T. J. Schaafsma, J. Mater. Chem. (in press)
[25] C. H. M. Marée, A. Kleinpenning, A. M. Vredenberg, and F. H. P. M. Habraken, Nucl. Instrum. Methods Phys. Res. B (in press).
[26] C. H. M. Marée, T. J. Savenije, T. J. Schaafsma, and F. H. P. M. Habraken, Appl. Surf. Sci. **93**, 291 (1996).
[27] N. F. Mott and E. A. Davis, *Electronic Processes in Non-Crystalline Materials* (Clarendon, Oxford, 1979).
[28] A. Désormeaux, J. J. Max, and R. M. Leblanc, J. Phys. Chem. **97**, 6670 (1993).
[29] *CRC Handbook of Chemistry and Physics*, edited by R. C. Weast, M. J. Astle, and W. H. Beyers (CRC, Boca Raton, FL, 1983).
[30] B. A. Gregg, M. A. Fox, and A. J. Bard, J. Phys. Chem. **94**, 1586 (1990).
[31] P. G. Schouten, Ph.D. thesis, Delft University, 1992.
[32] V. Balzani, S. Campagna, G. Denti, A. Juris, S. Serroni, and M. Venturi, Sol. Energy Mater. Sol. Cells **38**, 159 (1995).